ELSEVIER

Biochimica et Biophysica Acta 1454 (1999) 191–200

BIOCHIMICA ET BIOPHYSICA ACTA

BBA

www.elsevier.com/locate/bba

The effect of prolonged iron loading on the chemical form of iron oxide deposits in rat liver and spleen

Wanida Chua-anusorn [a], John Webb [a], David J. Macey [a], Pauline de la Motte Hall [b], Timothy G. St. Pierre [c,*]

[a] *Division of Science, Murdoch University, Murdoch, W.A. 6150, Australia*
[b] *Histopathology Department, Flinders Medical Centre, Bedford Park, S.A. 5042, Australia*
[c] *Department of Physics, The University of Western Australia, Nedlands, W.A. 6907, Australia*

Received 29 March 1999; accepted 31 March 1999

Abstract

Female Porton rats were loaded with iron either by supplementing the diet with 2.5% carbonyl iron for up to 22 months (18 rats) or by regularly injecting rat blood cells intraperitoneally for up to 10 months (eight rats). ^{57}Fe Mössbauer spectroscopy of freeze-dried samples of liver and spleen was used to analyse the chemical forms of iron deposited in these tissues over the period of iron loading. A sextet signal in the Mössbauer spectra was identified as being due to a form of haemosiderin based on the structure of the mineral goethite. The spectral parameters of the sextet signal in the rat tissues indicate that the goethite-like haemosiderin particles are less crystalline than those found in iron-loaded human tissues. For the dietary-iron-loaded rat livers, the fraction (F_s) of the Mössbauer signal in the form of this sextet was found to increase significantly (from approx 0.04 to 0.09) with the age of the rats ($r = 0.77$, $P < 0.0005$). This indicates that the fraction of liver iron in the form of the goethite-like haemosiderin increases with age of the rat and hence with the duration of iron loading. In addition, F_s for these livers was found to increase significantly with the fraction of iron in non-parenchymal cells as measured by computer-assisted morphometric analysis of histological sections ($r = 0.71$, $P < 0.005$).

Keywords: Iron overload; Mössbauer spectroscopy; Ferrihydrite; Hemosiderin; Liver; Spleen

1. Introduction

Iron overload in human tissues can result from several different causes. The two most common diseases associated with iron overload are genetic haemochromatosis and thalassaemia. Genetic haemochromatosis [1,2] results in iron overload caused by excess absorption of iron from the diet through the intestinal tract. Thalassaemia, a genetic disease caused by defective haemoglobin synthesis [3,4], results in iron overload either because of repeated blood transfusions [4] which are administered in order to alleviate the anaemia associated with the disease or, in the case of patients who do not receive regular blood transfusions, because of increased absorption of iron from the diet [5]. In all types of iron overload iron is deposited in the organs of the body in the form of ultrafine (nanometre scale) particles of iron(III) oxyhydroxide associated with haemosiderin and ferritin [6]. However, several case studies have

* Corresponding author. Fax: +61 (8) 93801014; E-mail: stpierre@physics.uwa.edu.au

0925-4439/99/$ – see front matter
PII: S0925-4439(99)00036-8

shown that at least three different chemical forms of iron(III) oxyhydroxide can be deposited in tissues and that the form of iron deposited may be disease-specific [7–12]. The three chemical forms have been identified as (i) ferrihydrite ($5Fe_2O_3 \cdot 9H_2O$), (ii) a goethite-like form of iron(III) oxyhydroxide, and (iii) a highly hydrated non-crystalline form of iron(III) oxyhydroxide.

The chemical forms of iron(III) oxyhydroxide deposited may well be related to the mechanisms of formation which may, in turn, be related to a combination of many factors [12]. These factors possibly include the extent of iron deposition and the route and duration of iron loading. In addition, the tissues in which the iron deposit is formed and the different cell types within that tissue may well play a role in the formation of these different chemical forms of iron oxyhydroxides. In mammals, the two dominant cell types associated with the storage of excess iron are the reticuloendothelial cells (RE cells) and parenchymal cells, the latter being represented mainly by hepatocytes.

In an attempt to identify the factors related to the different chemical forms of iron oxyhydroxide deposited in various disease states, an iron-loaded animal model was established [13]. The model was based on an earlier model [14] but was modified so that, over a prolonged time period, levels of iron loading similar to those found in human disease states (without chelation therapy) could be obtained. In order to determine whether the route of iron entry into the body affects the form of iron oxide ultimately deposited, two routes of administration were chosen. The first involved the prolonged administration of red blood cells injected via an intraperitoneal route, while the second involved the gastrointestinal administration of iron via dietary supplementation. Here we report on the form of the resulting iron oxyhydroxide deposits in the liver and spleen following the two routes of loading.

2. Materials and methods

2.1. Experimental rats

Female Porton rats, the offspring of mothers which had been iron-loaded during pregnancy and lactation with 2.5% carbonyl iron dietary supplementation, were used for all experimental procedures. Immediately after weaning (i.e. at 1 month after birth), rats were loaded with iron either via supplementation of the diet with 2.5% carbonyl iron (w/w) (18 rats) or via regular intraperitoneal blood injections (eight rats). Intraperitoneal injections of packed red blood cells (2 ml per 100 g body weight) were given weekly from 1 month after birth to 4 months after birth. Thereafter, the injection regime was changed to 4 ml of packed red cells per 100 g body weight at 2-week intervals. Full details of these procedures have been reported elsewhere [13]. The animals used in this study are the same animals that were used in previously reported work [13]. Animals ($n = 14$) from the dietary-iron-loaded group were killed at 2, 4, 6, 8, 11, 11.5, 14.5, 15, 18.5, 19, 21, 21.5, 22 or 22 months after birth. At 22 months after birth, dietary iron supplementation to the four remaining rats ceased and they were returned to a regular diet for 2, 4, 6 or 8 weeks, and thus were killed at 22.5, 23, 23.5 or 24 months after birth respectively. Rats from the parenteral-iron-loaded group were killed at 2, 4, 6, 8, 10 or 12 months after birth. In addition, injections to two rats were stopped at 10 months after birth, the rats being killed at 11 and 12 months after birth. All animals were killed using a 20% O_2 and 80% CO_2 gas mixture. All animal experimentation was conducted following procedures approved by Murdoch University Animal Ethics Committee (Permit 386R).

2.2. Tissue iron measurement

Following death, the liver and spleen from each rat were removed and rinsed with isotonic saline (0.9% NaCl) to remove excess blood. A small sample of each organ was removed for routine histological processing in order to measure the fraction of iron in non-parenchymal cells using computer-assisted morphometric analysis. Computer image analysis of histological sections has previously been used to measure the stainable hepatic iron in non-parenchymal cells in Perls' stained histological liver sections of these rats [13].

Following the removal of material for light microscopy, the remaining portions of the liver and spleen from each rat were quickly freeze-dried. Each freeze-

dried sample was then ground to a powder to ensure mixing and sub-samples were taken for atomic absorption spectroscopy and Mössbauer spectroscopy.

2.3. Mössbauer spectroscopy

Mössbauer spectra were recorded using a ^{57}Co in Rh foil source (approximately 25 mCi) mounted on a constant acceleration drive. Samples were held at a temperature of 78 K using a liquid nitrogen cryostat. The source was scanned over the velocity range −13 to +13 mm s^{-1} with a double ramp waveform. Spectra were subsequently folded to eliminate the parabolic background due to the variation in the solid angle subtended by the detector window about the source. The resulting Mössbauer spectra consisted of 250 data points with a background count of between 2×10^6 and 40×10^6 counts per channel. The counting time was determined by the properties of the sample under study. The velocity scale was calibrated with reference to the spectrum of an α-iron foil at room temperature, the centre of the spectrum being taken as zero velocity. The ground freeze dried tissue samples were packed into 10 mm diameter perspex sample holders for Mössbauer spectroscopy. The sample thickness was adjusted, whenever possible, so that the intensity of the 14.4 keV γ-rays was attenuated by a factor of approximately 1/e by the sample. In several cases, especially with the younger rats, insufficient sample was available (due to smaller organs) to attain this optimum thickness and so thinner samples were used.

Each Mössbauer spectrum was initially fitted with a doublet and sextet of Lorentzian peaks using a sum of squares minimisation procedure. This fitting procedure yields satisfactory spectral parameters and doublet to sextet area ratios for spectra with high signal-to-noise ratios. However, for spectra with low sextet signal-to-noise ratios, the fitting procedure tended to give unreliable results as described elsewhere [12] and hence the following procedure was adopted.

Mean values for the Mössbauer spectral parameters (Table 1) of the sextet signals in the 11 spectra of the dietary-iron-loaded rat livers with the highest sextet signal-to-noise ratio were used as a standard with which to refit all of the rat tissue spectra. All of the spectra were fitted with a high-spin iron(III) doublet and the standard sextet. The linewidths (Γ), magnetic hyperfine field splitting (B_{hf}), centre shift (δ), and quadrupole perturbation (ΔE_Q) of the sextet were allowed to vary from the mean values derived from the 11 spectra with the highest sextet signal-to-noise ratios by up to one standard deviation. The area of the sextet was allowed to vary freely. In this way, the relative spectral area of the sextet in spectra with very low sextet signal-to-noise ratios could be more reliably assessed, assuming that the Mössbauer spectral parameters of the sextet do not vary significantly from sample to sample.

In order to gauge the magnitude of the error in measurement of the relative spectral area of the sextet component in the spectra, the spectra were also analysed in terms of the total numbers of counts within particular velocity regions of interest [12]. Three regions of interest were identified by inspection of the 11 spectra of the dietary-iron-loaded rat livers with the highest sextet signal-to-noise ratio. The three regions represent (i) velocity regions where the Mössbauer signal is negligible (i.e. background), (ii) velocity regions encompassing almost all of the outer peaks of the sextet without encompassing any

Table 1
Mean values with standard deviations or ranges for Mössbauer spectral parameters of the sextet components in dietary-iron-loaded rat livers and thalassemic human tissues at 78 K

Tissue	δ	ΔE_Q	B_{hf}	Γ
Rat livers ($n=11$)	0.53 (0.18)	−0.31 (0.33)	46.2 (0.9)	1.25 (0.52)
Human thalassaemic spleen ($n=4$)	0.47 (0.42 to 0.51)	−0.21 (−0.28 to −0.13)	47.0 (46.5 to 47.4)	0.86 (0.73 to 0.99)
Human thalassaemic liver ($n=4$)	0.51 (0.48 to 0.56)	−0.30 (−0.34 to −0.27)	46.7 (46.5 to 47.0)	0.81 (0.60 to 1.09)
Human thalassaemic pancreas ($n=3$)	0.43 (0.35 to 0.49)	−0.10 (−0.29 to 0.24)	46.7 (46.6 to 46.8)	0.86 (0.74 to 1.10)

The human tissue data are taken from [12].
δ is the centre shift in mm s^{-1}. ΔE_Q is the quadrupole perturbation on the magnetic hyperfine field splitting. B_{hf} is the magnetic hyperfine field splitting in T. Γ is the full linewidth at half height of the outer lines of the sextet in mm s^{-1}.

significant intensity from other parts of the spectrum, and (iii) the entire velocity range of the spectrum. These regions of interest can be defined by four velocity boundaries which were found by inspection to be $v_1 = -9.2$ mm s^{-1}, $v_2 = -5.3$ mm s^{-1}, $v_3 = 6.2$ mm s^{-1} and $v_4 = 9.75$ mm s^{-1}, where region 1 is $v < v_1$ and $v > v_4$, region 2 is $v_1 < v < v_2$ and $v_3 < v < v_4$, and region 3 is the entire velocity scan of the spectrum ($v_{min} < v < v_{max}$). If c_i is the number of data channels in region i, X_i is the total number of counts expected in region i if the intensity of the Mössbauer signal were zero, and $S_i = B_i - X_i$ (i.e. the number of counts missing in region i due to the presence of the Mössbauer signal) then the fractional area of the spectrum in the sextet is given by

$$F_S = \frac{2S_2}{S_3} \pm \frac{2S_2}{S_3}\left[\frac{\left(\frac{c_2^2 X_1}{c_1^2} + X_2\right)}{S_2^2} + \frac{\left(\frac{c_3^2 X_1}{c_1^2} + X_3\right)}{S_3^2}\right]^{1/2} \quad (1)$$

assuming that the ratio of areas of the outer to middle to inner pairs of lines in a sextet is 3:2:1 and that any signal in region 2 is solely due to a sextet similar to the ones observed in the spectra with high sextet signal-to-noise ratios. The error expression in Eq. 1 is obtained by commutation of Poisson statistical errors of counting in each region of interest.

Thus this method of analysis gives an indication of both the fraction of spectral intensity in the form a sextet in the Mössbauer spectrum of the rat tissues and the inherent error on the measurement of this fraction due to the Poisson statistics of counting. This is particularly useful when the sextet signal-to-noise ratio is very low.

3. Results

The iron content of the liver and spleen tissues and the morphometric measurement of the fraction of iron in non-parenchymal cells correlated well with the duration of iron loading of the rats. In addition, the fraction of iron in non-parenchymal cells was found to be less in the parenteral-iron-loaded group. These results have been shown in detail elsewhere [13].

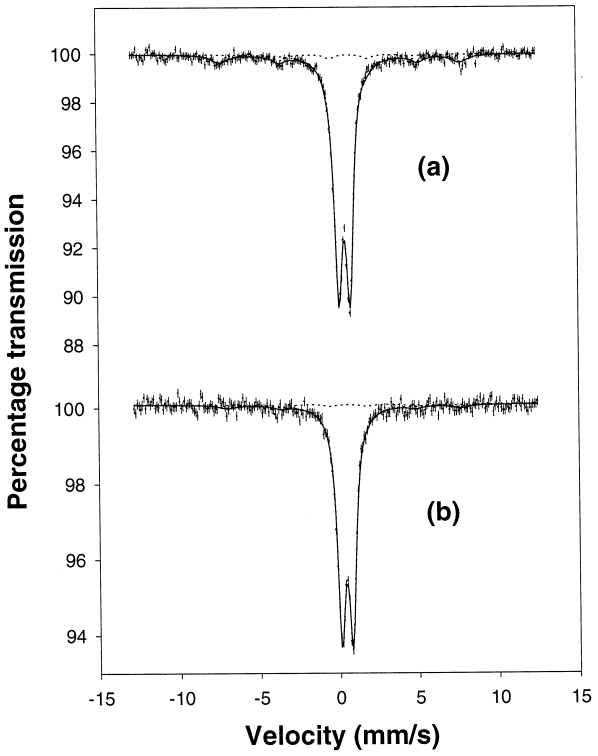

Fig. 1. Mössbauer spectra of (a) liver tissue and (b) spleen tissue from a dietary-iron-loaded rat. Spectra were recorded with sample temperatures of 78 K. The error bars on the data points are given by the square root of the number of γ-ray counts for each data point. The solid curves are least squares fits of the central doublet and standard sextet components to the spectrum (see Section 2). The dotted curves indicate the two spectral subcomponents comprising the fit.

Mössbauer spectra of the livers and spleens from both iron-loaded groups of rats consisted of a relatively intense central doublet (Figs. 1 and 2) with spectral parameters indicative of paramagnetic or superparamagnetic high-spin iron(III) (Table 2). Many of the spectra also clearly showed a small sextet signal (Figs. 1a and 2b). No signal due to haem iron could be detected in spectra of either livers or spleens. Mean values and standard deviations for the spectral parameters of the doublet are shown in Table 2.

3.1. Dietary-iron-loaded rats

3.1.1. Liver

The fraction (F_s) of the Mössbauer spectrum in the form of a sextet for the liver was found to increase

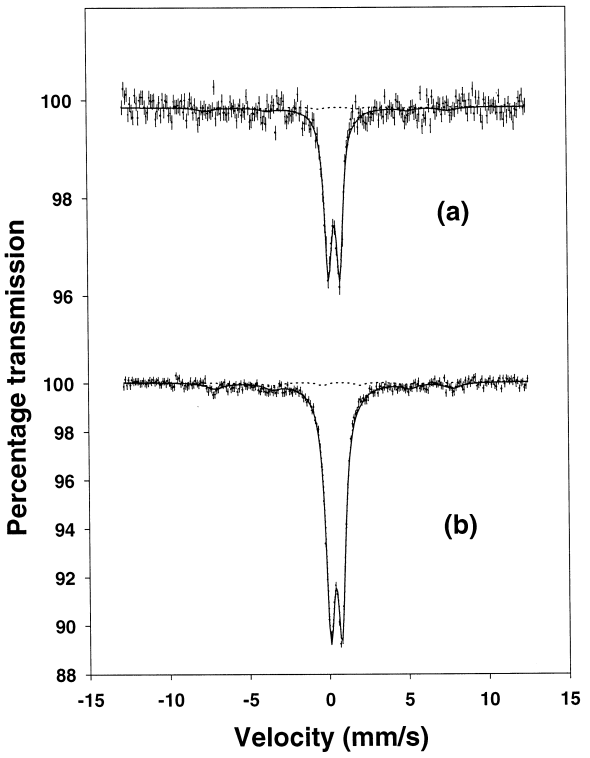

Fig. 2. Mössbauer spectra of (a) liver tissue and (b) spleen tissue from a parenteral-iron-loaded rat. Spectra were recorded with sample temperatures of 78 K. The error bars on the data points are given by the square root of the number of γ-ray counts for each data point. The solid curves are least squares fits of the central doublet and standard sextet components to the spectrum (see Section 2). The dotted curves indicate the two spectral subcomponents comprising the fit.

significantly with the age of the rats (Fig. 3) with a Spearman rank-order correlation coefficient of 0.77 ($P < 0.0005$). No significant change in the trend was observed after the rats were transferred to the non-iron-enriched diet. A significant correlation between F_s and tissue iron concentration was not found ($r = 0.41$, $P = 0.10$).

In addition, F_s for the liver was found to increase significantly with the fraction of iron in non-parenchymal cells as measured by computer assisted morphometric analysis (Fig. 4) with a Spearman rank-order correlation coefficient of 0.71 ($P < 0.005$).

3.1.2. Spleen

The distribution of quadrupole splittings (Table 2) for the doublets was found to be significantly different from that for the dietary-iron-loaded rat livers (Kolmogorov-Smirnov (K-S) statistic of 0.69, $P < 0.001$). No significant correlation was found between F_s and either duration of iron loading or tissue iron concentration. The mean value of F_s was measured to be 0.059 with a standard deviation of 0.03.

3.2. Parenteral-iron-loaded rats

3.2.1. Livers

The distribution of quadrupole splittings for the doublets (Table 2) was found to be significantly different from that for the dietary-iron-loaded rat livers

Table 2
Mean values (with standard deviations or ranges) for Mössbauer spectral parameters of the central doublet components for rat and human tissues at 78 K

Tissue	δ	ΔE_Q	Γ
Dietary-iron-loaded rats			
livers ($n = 17$)	0.442 (0.004)	0.711 (0.009)	0.603 (0.037)
spleens ($n = 16$)	0.447 (0.008)	0.681 (0.035)	0.578 (0.051)
Parenteral-iron-loaded rats			
livers ($n = 8$)	0.438 (0.006)	0.683 (0.035)	0.572 (0.044)
spleens ($n = 8$)	0.438 (0.008)	0.715 (0.008)	0.622 (0.029)
Human tissues			
Thai β-thal/Hb E spleens ($n = 12$)	0.46 (0.02)	0.66 (0.03)	0.61 (0.06)
Australian β-thal spleens ($n = 7$)	0.46 (0.03)	0.68 (0.03)	0.67 (0.08)
Normal spleens ($n = 12$)	0.39 (0.09)	0.51 (0.10)	0.56 (0.14)
Thai β-thal/Hb E livers ($n = 4$)	0.48 (0.47–0.49)	0.66 (0.64–0.70)	0.58 (0.53–0.68)
Normal livers ($n = 12$)	0.45 (0.06)	0.60 (0.10)	0.64 (0.16)
Thai β-thal/Hb E pancreas ($n = 3$)	0.47 (0.47–0.48)	0.64 (0.60–0.66)	0.58 (0.52–0.62)

The data for human tissues (from Thai β-thalassaemia/haemoglobin E patients, Australian β-thalassaemia patients and normal subjects) are taken from [12] and [24].
δ is the centre shift in mm s^{-1}. ΔE_Q is the quadrupole splitting in mm s^{-1}. Γ is the full linewidth at half height in mm s^{-1}.

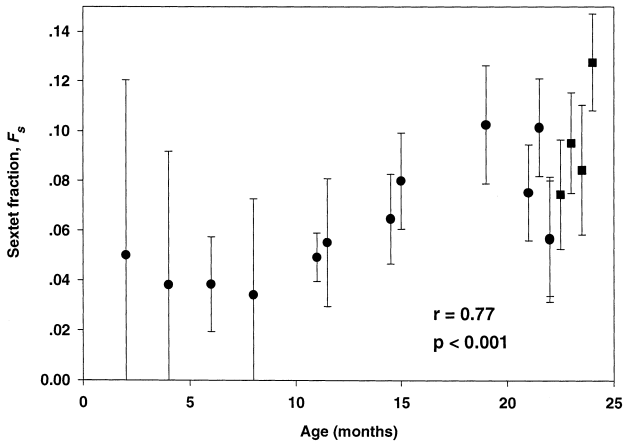

Fig. 3. Fraction (F_s) of Mössbauer spectrum in the form of sextet for dietary-iron-loaded rat liver tissue at 78 K against age of rat. Note that the iron supplementation to the diet was stopped after 22 months. The error bars are calculated from Eq. 1. Square symbols indicate rats that had been on an unsupplemented diet from age 22 months onwards.

(K-S statistic of 0.63, $P < 0.02$). No significant correlation was found between F_s and either duration of iron loading, tissue iron concentration, or fraction of iron in non-parenchymal cells as measured by computer assisted morphometric analysis. The mean value of F_s was measured to be 0.09 with a standard deviation of 0.07.

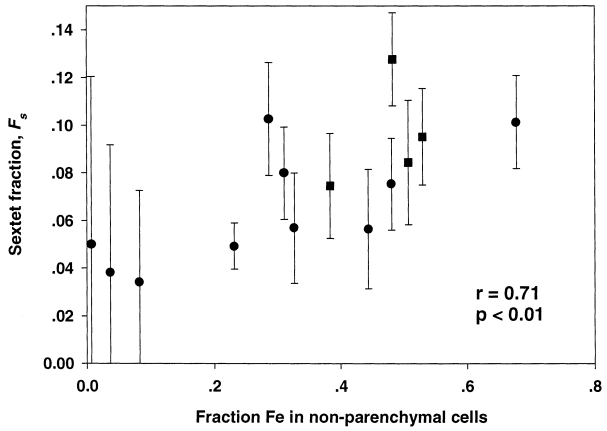

Fig. 4. Fraction (F_s) of Mössbauer spectrum in the form of sextet for dietary-iron-loaded rat liver tissue at 78 K against fraction of iron in non-parenchymal cells. The error bars are calculated from Eq. 1. Square symbols indicate rats that had been on unsupplemented diet from age 22 months onwards.

3.2.2. Spleen

The distribution of quadrupole splittings (Table 2) for the doublets was found to be significantly different from those for both the dietary-iron-loaded rat spleens (K-S statistic of 0.88, $P < 0.0005$) and parenteral-iron-loaded rat livers (K-S statistic of 0.63, $P < 0.05$). In addition, the distribution of linewidths (Table 2) for the doublets was found to be significantly different from those for both the dietary-iron-loaded rat spleens (K-S statistic of 0.63, $P < 0.02$) and parenteral-iron-loaded rat livers (K-S statistic of 0.63, $P < 0.05$).

No significant correlation was found between F_s and either duration of iron loading or tissue iron concentration.

3.3. Error analysis

In order to obtain an approximate estimate of the error on each measurement of F_s, each spectrum was analyzed in terms of the total number of counts accumulated in three regions of the spectrum giving an alternative measure of F_s and an estimate for the error on F_s, ΔF_s (see Section 2). Fig. 5 shows a plot of the calculated error on F_s for samples with different F_s and concentrations of iron. Although the

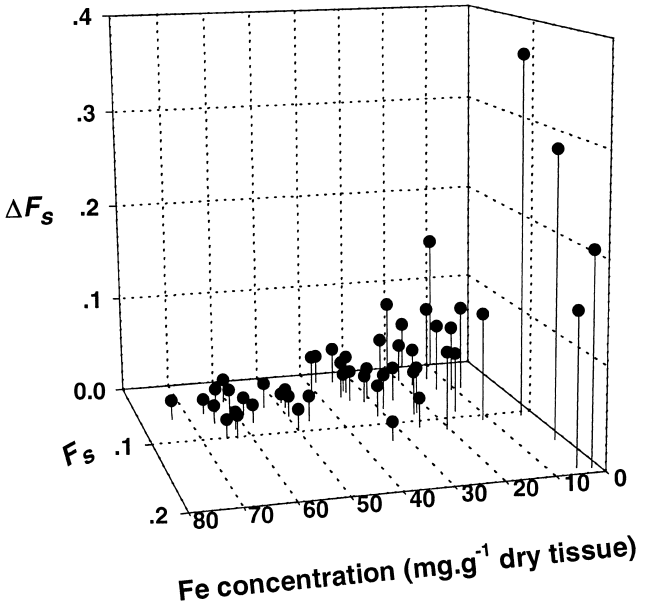

Fig. 5. The calculated error (ΔF_s) on the fraction (F_s) of the Mössbauer spectrum in the form of sextet against iron concentration and F_s for all rat tissues in this study.

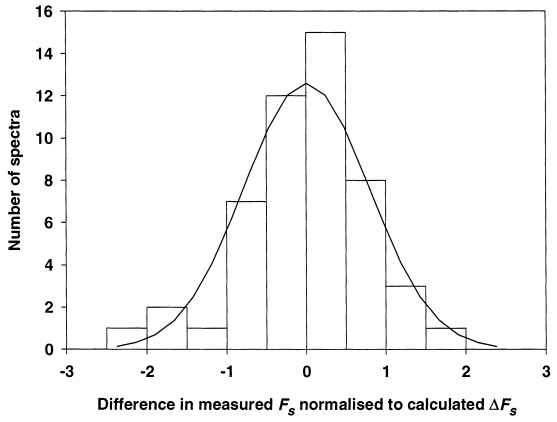

Fig. 6. Histogram showing the distribution of differences between the value of F_s (normalised to the calculated ΔF_s) measured by (i) fitting the standard sextet to the spectrum and by (ii) the region of interest method. The curve is a fit of a normal distribution to the data.

errors can be reduced to some extent by extending the counting time in the experiments, there is a practical limit to the time for one measurement (approximately 1 week). The exponent of 1/2 in Eq. 1 results in diminishing returns in error reduction for longer counting times. The trends in Fig. 5 are as expected, with smaller errors for higher concentrations of iron and larger values of F_s. Fig. 6 shows the distribution of differences (each normalised to the calculated error, ΔF_s) in the measurement of F_s between the two methods for all of the rat tissues in the study. The distribution approximates well to a normal distribution. The mean of the distribution is 0.00 (S.D. ± 0.79). This indicates that ΔF_s calculated from Eq. 1 is a reasonable estimate for the random errors on the measurement of F_s.

4. Discussion

The major component in all of the Mössbauer spectra of the rat tissues was a central doublet with parameters indicative of high-spin iron(III) in either a paramagnetic or superparamagnetic form. A minor sextet component due to magnetic hyperfine field splitting of the ^{57}Fe nuclear energy levels (Table 1) was also present with varying degrees of relative intensity. The fact that signals due to haem iron were not detectable in any of the spectra may be due to the elimination of excess blood by rinsing the organs with 0.9% NaCl solution after organ removal.

Similar central doublet and sextet signals have been observed in previous reports of Mössbauer spectra of human tissues or human tissue extracts [6,8–12,15–25]. On the basis of these previous reports, these spectral components can be identified as being due to polynuclear iron(III) oxyhydroxide deposits in the tissues. This is consistent with the fact that the predominant form of iron found in iron-loaded tissues is usually haemosiderin [26]. The doublet component in the spectrum has parameters consistent with (a) ferritin, (b) non-crystalline haemosiderin, (c) haemosiderin based on the structure of the mineral ferrihydrite, or (d) the doublet component associated with haemosiderin based on the structure of the mineral goethite (the doublet component being due to those haemosiderin particles with a smaller magnetic anisotropy energy) [6–8]. As such it is not possible to unambiguously identify the source of this signal and indeed the signal may be due to a combination of all or any the above forms of iron. However, the sextet component in the spectrum can be identified as being due to the presence of a haemosiderin which is based on the structure of the mineral goethite, since this is the only form of mammalian tissue iron deposit known to give a Mössbauer spectral sextet component with these parameters at 78 K [9,10,25].

Previous Mössbauer spectroscopy studies of rat organs have revealed only the central doublet component at 78 K [17,19,25,27–30]. However, none of these previous studies involved loading the rats with iron for the same length of time or to the same extent as in the present study. This is the first study to have identified the goethite-like form of haemosiderin in rat tissues which strongly suggests that degree of iron loading and/or duration of iron loading and/or age may be determining factors in the formation of this type of haemosiderin since the rats in this study have been iron-loaded to higher levels and longer periods than all previous studies.

The Mössbauer spectra in this study revealed significant differences in the quadrupole splitting distributions of the central doublet between the groups of organs studied. The quadrupole splitting distributions for the dietary-iron-loaded rat livers and paren-

teral-iron-loaded rat spleens were centred around higher values and were narrower than those for the dietary-iron-loaded rat spleens and parenteral-iron-loaded rat livers. In addition, the linewidths of the doublets for the parenteral-iron-loaded rat spleens were distributed with significantly larger values than those for the dietary-iron-loaded rat spleens and parenteral-iron-loaded rat livers. Larger quadrupole splittings indicate a less symmetric environment for the ^{57}Fe nucleus. This could be caused by increased disorder in the iron oxyhydroxide particles. Vacancies, invaginations, fractal surfaces, and dislocations would all contribute to an increased quadrupole splitting due to the asymmetric environments at these structural defects. They would also result in increased linewidths due to the increased variation in microenvironments in the structure of the particles. These effects have been observed in previous Mössbauer spectral studies on ferrihydrites with different degrees of crystallinity, which demonstrated that lower degrees of crystallinity resulted in doublets with larger quadrupole splittings and linewidths [31]. Thus, these data imply that the iron oxyhydroxide particle structures contributing to the doublet component in the Mössbauer spectra of the rat livers and spleens are more disordered in the dietary-iron-loaded rat livers and parenteral-iron-loaded rat spleens than they are in the dietary-iron-loaded rat spleens and parenteral-iron-loaded rat livers. The greater degree of disorder could be related to the more rapid rate of iron deposition observed in the dietary-iron-loaded rat livers and parenteral-iron-loaded rat spleens [13].

It is worth noting the rather small standard deviations in the Mössbauer spectral parameters of the central doublets for the rat tissues (Table 2) when compared with those obtained for human tissues [12]. This suggests that the rat system is a rather good model in that it gives reproducible results in comparison with human tissues. The larger standard deviations for the spectral parameters of the central doublet for the human tissues are presumably a result of patient variability. Note that there may be a systematic error in the normal human spleen tissue Mössbauer spectral parameters [12,24] because of the presence of a fraction of the spectrum in the form of a haem iron signal in some of the spectra. This would have complicated the fitting procedure and may explain the somewhat extreme values measured for these spectral parameters.

The mean spectral parameters for the sextet (Table 1) derived from free fits to the 11 spectra of dietary-iron-loaded rat livers with the highest sextet signal-to-noise ratio were similar to those found for thalassemic human spleen, liver, and pancreas tissue [12]. However, the slightly lower magnetic hyperfine field splittings and larger linewidths may indicate that the degree of crystallinity of the iron oxyhydroxide contributing to this spectral component is less than that in the human tissues. This may be related to either the rate of deposition of iron or aging of the iron oxyhydroxide deposits. Aging of iron oxyhydroxide systems can lead to increased crystallinity [32,33]. The human tissues were typically 10–20 years old compared to the age of less than 2 years for the rat tissues.

The positive correlation of F_s for the dietary-iron-loaded rat livers with the age and duration of iron loading of the rats (Fig. 2) suggests that either processes are converting the ferrihydrite-like form of iron oxyhydroxide into the goethite-like form with time or that different iron oxide deposition mechanisms are involved during the life of the rat.

The positive correlation of F_s with the fraction of iron deposited in the non-parenchymal cells of the liver suggests that the formation of the goethite-like iron oxyhydroxide deposits may be associated with the non-parenchymal cells. However, experiments involving the physical separation of the non-parenchymal cells will need to be carried out before this can be confirmed.

Acknowledgements

This work was partly funded by the National Health and Medical Research Council.

References

[1] J.N. Feder, A. Gnirke, W. Thomas, Z. Tsuchihashi, D.A. Ruddy, A. Basava, F. Dormishian, R. Domingo, M.C. Ellis, A. Fullan et al., A novel MHC classI-like gene in patients with hereditary haemochromatosis, Nature Genet. 13 (1996) 399–408.

[2] L.W. Powell, E.C. Jazwinska, Hemochromatosis in heterozygotes, New Engl. J. Med. 335 (1996) 1837–1839.
[3] D.R. Higgs, The talassaemia syndromes, Q. J. Med. 86 (1993) 559–564.
[4] N.F. Olivieri, G.M. Brittenham, Iron-chelating therapy and the treatment of thalassaemia, Blood 89 (1997) 739–761.
[5] P. Pootrakul, S. Hungspenges, S. Fucharoen, D. Baylink, E. Thompson, E. English, M. Lee, J. Burnell, C. Finch, Relation between erythopoiesis and bone metabolism in thalassaemia, New Engl. J. Med. 304 (1981) 1470–1473.
[6] T.G. St. Pierre, J. Webb, S. Mann, Ferritin and hemosiderin: structural and magnetic studies of the iron core, in: S. Mann, J. Webb, R.J.P. Williams (Eds.), Biomineralization: Chemical and Biochemical Perspectives, VCH, Weinheim, 1989, pp. 295–344.
[7] S. Mann, V.J. Wade, D.P.E. Dickson, N.M.K. Reid, R.J. Ward, M. O'Connell, T.J. Peters, Structural specificity of haemosiderin iron cores in iron-overload diseases, FEBS Lett. 234 (1988) 69–72.
[8] D.P.E. Dickson, N.M.K. Reid, S. Mann, V.J. Wade, R.J. Ward, T.J. Peters, Mössbauer spectroscopy, electron microscopy and electron diffraction studies of the iron cores in various human and animal haemosiderins, Biochim. Biophys. Acta 957 (1988) 81–90.
[9] T.G. St. Pierre, K.C. Tran, J Webb, D.J. Macey, P. Pootrakul, D.P.E. Dickson, Core structures of haemosiderins deposited in various organs in β-thalassemia/haemoglobin E disease, Hyperfine Interact. 71 (1992) 1279–1282.
[10] T.G. St. Pierre, K.C. Tran, J. Webb, D.J. Macey, P. Pootrakul, Mineralization of iron in ferritin and haemosiderin: the effect of tissue environment on mineral structure, in: S. Suga (Ed.), Mechanisms and Phylogeny of Mineralization in Biological Systems, Springer-Verlag, Tokyo, 1991, pp. 291–295.
[11] J. Webb, T.G. St. Pierre, D.J. Macey, K.C. Tran, P. Pootrakul, Effect of β-thalassemia/hemoglobin E disease on the structure of biogenic ferrihydrite deposits in iron-loaded human heart and spleen ferritins, Catena Suppl. 21 (1992) 169–178.
[12] T.G. St. Pierre, W. Chua-anusorn, J. Webb, D. Macey, P. Pootrakul, The form of iron oxide deposits in thalassemic tissues varies between different groups of patients: a comparison between Thai β-thalassemia/hemoglobin E patients and Australian β-thalassemia patients, Biochim. Biophys. Acta 1407 (1998) 51–60.
[13] W. Chua-anusorn, D.J. Macey, J. Webb, P.d.l.M. Hall, T.G. St. Pierre, Effects of prolonged iron loading in the rat using both parenteral and dietary routes, BioMetals (1999) (in press).
[14] J. Olynyk, M. Mackinnon, W. Reed, P. Willams, R. Kerr, P. Hall, A long term study of the interaction of iron and alcohol in an animal model of iron overload, Hepatology 15 (1992) 502–506.
[15] K.S. Kaufman, G.C. Papaefthymiou, R.B. Frankel, A. Rosenthal, Nature of iron deposits on the cardiac walls in β-thalassemia by Mössbauer spectroscopy, Biochim. Biophys. Acta 629 (1980) 522–529.
[16] S.H. Bell, M.P. Weir, D.P.E. Dickson, J.F. Gibson, G.A. Sharp, T.J. Peters, Mössbauer spectroscopic studies of human haemosiderin and ferritin, Biochim. Biophys. Acta 787 (1984) 227–236.
[17] J.N. Rimbert, F. Dumas, C. Kellershohn, R. Girot, P. Brissot, Mössbauer spectroscopy study of iron overloaded livers, Biochimie 67 (1985) 663–668.
[18] J.N. Rimbert, F. Dumas, G. Richardot, C. Kellershohn, Magnetic and quadrapolar studies of the iron storage overload in livers, Hyperfine Interact. 29 (1986) 1439–1442.
[19] T.G. St. Pierre, D.P.E. Dickson, J.K. Kirkwood, R.J. Ward, T.J Peters, A Mössbauer spectroscopic study of the form of iron in iron-overload, Biochim. Biophys. Acta 924 (1987) 447–451.
[20] T.G. St. Pierre, D.P.E. Dickson, D.H. Jones, Thalassaemic human spleen ferritin and haemosiderin in applied magnetic fields, Hyperfine Interact. 42 (1988) 917–920.
[21] M. Chorxy, R. Meczynski, T.J. Panek, Mössbauer effect study of liver tissues, J. Radioanal. Nucl. Chem. Lett. 128 (1988) 201–206.
[22] D.P.E. Dickson, R.K. Pollard, B. Borch-Iohnsen, R.J. Ward, T.J. Peters, Mössbauer spectroscopic studies of haemosiderins from different sources, Hyperfine Interact. 42 (1988) 889–892.
[23] J. Webb, T.G. St. Pierre, K.C. Tran, W. Chua-anusorn, D.J. Macey, P. Pootrakul, Biologically significant iron(III) oxyhydroxy polymers: Mössbauer spectroscopic study of ferritin and hemosiderin in pancreas tissue of β-thalassemia/hemoglobin E disease, Inorg. Chim. Acta 242-243 (1996) 121–125.
[24] W. Chua-anusorn, T.G. St. Pierre, J. Webb, D.J. Macey, P. Yansukon, P. Pootrakul, Mössbauer spectroscopic study of the forms of iron in normal human liver and spleen tissue, Hyperfine Interact. 91 (1994) 905–910.
[25] R.J. Ward, M. Ramsey, D.P.E. Dickson, C. Hunt, T. Douglas, S. Mann, F. Aouad, T.J. Peters, R.R. Crichton, Further characterisation of forms of haemosiderin in iron-overloaded tissues, Eur. J. Biochem. 225 (1994) 187–194.
[26] M.P. Weir, J.F. Gibson, T.J. Peters, Hemosiderin and tissue damage, Cell Biochem. Func. 2 (1984) 186–194.
[27] L. May, J.L. Holtzman, Mössbauer spectroscopy of lyophilized rat liver microsomes, Biochem. Biophys. Res. Commun. 39 (1970) 296–300.
[28] B.K. Semin, A.A. Novakova, A.Y. Aleksandrov, I.I. Ivanov, Mössbauer spectroscopy of iron metabolism and iron intracellular distribution in liver of rats, Biochim. Biophys. Acta 715 (1982) 52–56.
[29] S.C. Andrews, M.C. Brady, A. Treffry, J.M. Williams, S. Mann, M.I. Clenton, W. de Bruijn, P.M. Harrison, Studies on haemosiderin and ferritin from iron-loaded rat liver, Biol. Metals 1 (1988) 33–42.
[30] R.J. Ward, A.L. Florence, D. Baldwin, C. Abiaka, F. Roland, M.H. Ramsey, D.P.E. Dickson, T.J. Peters, R.R. Crichton, Biochemical and biophysical investigations of the

ferrocene-iron-loaded rat: an animal model of primary haemochromatosis, Eur. J. Biochem. 202 (1991) 405–410.
[31] E. Murad, J.H. Johnston, Iron oxides and oxyhydroxides, in: G.J. Long (Ed.), Mössbauer Spectroscopy Applied to Inorganic Chemistry, Vol. 2, Plenum Press, New York, 1987, pp. 507–582.
[32] C.M. Flynn, Hydrolysis of inorganic iron(III) salts, Chem. Rev. 84 (1984) 31–41.
[33] R.M. Cornell, R. Giovanoli, W. Schneider, Review of the hydrolysis of iron(III) and the crystallization of amorphous iron(III) hydroxide hydrate, J. Chem. Tech. Biotechnol. 46 (1989) 115–134.